

## Steady-state sequences: Spoiled and balanced methods

Karla L Miller, FMRIB Centre, University of Oxford

### What is steady-state imaging?

In the context of MRI pulse sequences, the term “steady state” typically refers to the equilibrium condition that evolves when magnetization experiences a train of radiofrequency (RF) pulses. If RF pulses occur at broadly spaced intervals ( $TR \gg T1$ ), the magnetization recovers fully between pulses due to relaxation, and the steady-state is identical to the fully-relaxed magnetization,  $M_0$ . In general, though, RF pulses are applied sufficiently rapidly that the magnetization does not recover fully between pulses ( $TR < T1$ ), and the magnetization eventually develops a steady-state condition that is distinct from  $M_0$ . In this manuscript, we assume that both TR and flip angle ( $\alpha$ ) are constant throughout the pulse sequence.

For most MRI pulse sequences, TR is on the order of seconds, making it of similar magnitude to T1, but much longer than T2. In this case, at the end of the TR, the magnetization has decayed away completely in the transverse plane, but has not yet recovered fully along the longitudinal axis. The result is a “*longitudinal steady state*”, where the magnetization tipped away from the longitudinal axis by an RF pulse is exactly cancelled by recovery of magnetization along the longitudinal axis during the TR. Longitudinal steady states depend on the T1 of tissue, but not T2.

However, “*steady-state sequences*” commonly refer to a more specific case in which both T1 and T2 relaxation are interrupted by very rapid RF pulses ( $TR \leq T2 < T1$ ). In this situation, there is residual transverse magnetization at the end of the TR that will be tipped by the subsequent RF pulse. We would describe the result as a “*transverse steady state*” (with the understanding that this necessarily implies steady state of the longitudinal component, as well). Again, we can determine the steady state by imposing the equilibrium condition that the effects of relaxation and precession of the magnetization during the TR must be exactly cancelled by the RF pulse.

The signal dynamics of steady-state sequences are considerably more complicated than conventional sequences, and depend on T1, T2 and the phase (angle) between the magnetization and the axis of the RF pulse. In fact, it is the dependence of the steady state on phase that leads to the tremendous richness and flexibility of steady-state sequences, as well as many of the complications in dealing with these methods.

Steady-state sequences differ based on how the transverse magnetization is manipulated to influence contrast, and can be considered to fall into three categories: spoiled gradient echo (GRE), balanced steady-state free precession (SSFP) and unbalanced SSFP. Unfortunately, nomenclature is not standardized, and these sequences are also known by the names given in Table 1. Timing diagrams for the sequences discussed here are depicted in Figure 1.

Sequence	Alternate names	Description
Spoiled GRE	T1-FFE, FLASH, SPGR	Spoiled (usually RF spoiled)
SSFP-FID	FISP, FFE, FAST, GRASS,	Unbalanced gradient after readout
SSFP-Echo	PSIF, T2-FFE, CE-FAST	Unbalanced gradient before readout
Balanced SSFP	TrueFISP, Balanced FFE, FIESTA	Fully balanced (no net gradient)

**Table 1.** Steady-state sequences, alternate names and description, inspired by Chapter 14 in [5].

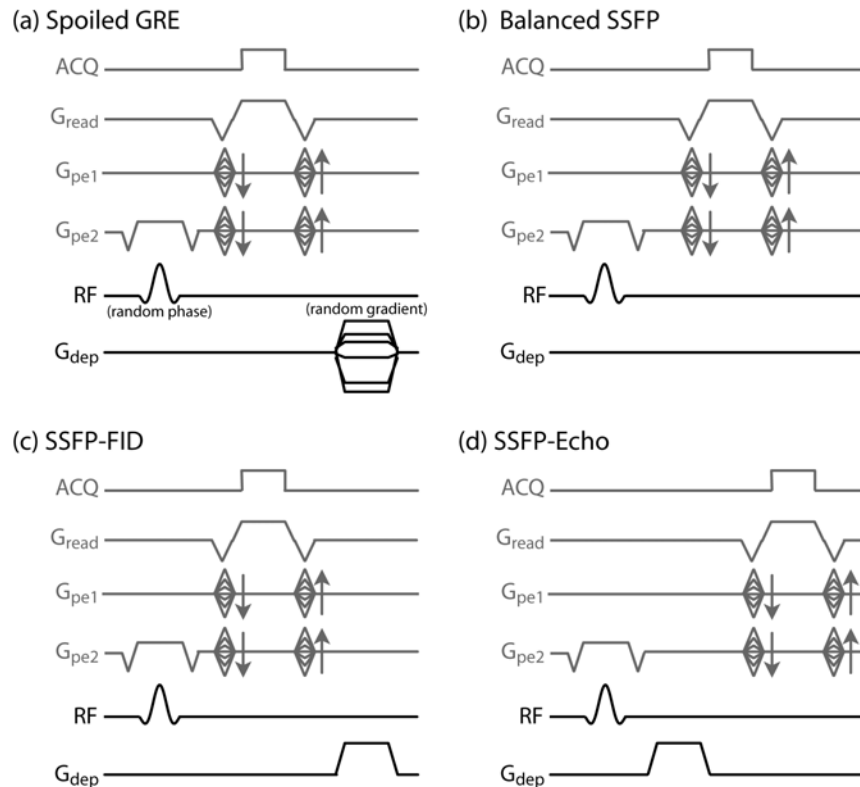


**Figure 1.** Sequence timing diagrams for the four steady-state sequences. The k-space readout (top lines, in gray) depict a 3D, single-line acquisition (3DFT); however, any readout can in general be used, provided it is refocused to have zero net gradient area at the end of the TR. The sequences differ in their dephasing gradient ( $G_{dep}$ ) and the RF phase. SSFP sequences are characterized by fixed RF phase and dephasing gradient, while spoiled sequences have randomized RF phase and/or dephasing gradient. The three SSFP sequences have: no dephasing gradient (balanced SSFP), a post-acquisition gradient (SSFP-FID) or a pre-acquisition gradient (SSFP-Echo). In order to understand the magnetization dynamics of each sequence, we need only consider the RF and dephasing gradient (bottom two lines).

### Spoiled sequences.

Spoiling aims to manipulate the residual magnetization that remains at the end of the TR such that it does not contribute signal in subsequent repetition periods. If this can be achieved, the signal will be a fairly pure T1 contrast [1]. However, the signal level will by definition be reduced compared to unspoiled sequences that do not attempt to remove the residual transverse signal. Spoiled sequences are typically used when the primary goal of using short TR is acquisition speed, rather than to exploit steady-state signal dynamics to achieve novel contrast.

**Gradient spoiling.** The easiest spoiling method to understand is gradient spoiling, in which a gradient pulse is used to create a range of phase angles across a voxel. This “dephasing” effect causes the transverse magnetization to self-cancel (see Figure 2a). However, these gradients have not destroyed the transverse magnetization, but simply suppressed its signal. If the same spoiling gradient is used every TR, a fraction of the dephased magnetization will be rephased to form a signal echo in later TRs (in fact, the use of a fixed gradient would make this an “unbalanced SSFP” sequence, described below). Proper gradient spoiling requires a randomized gradient each TR to avoid this rephasing. However, achieving a broad range of variable areas requires either very strong gradients or long TR, making this impractical under most circumstances. In addition, the quality of spoiling is spatially dependent, with no spoiling at the centre of the gradients [2]. These limitations make RF spoiling the preferred technique.

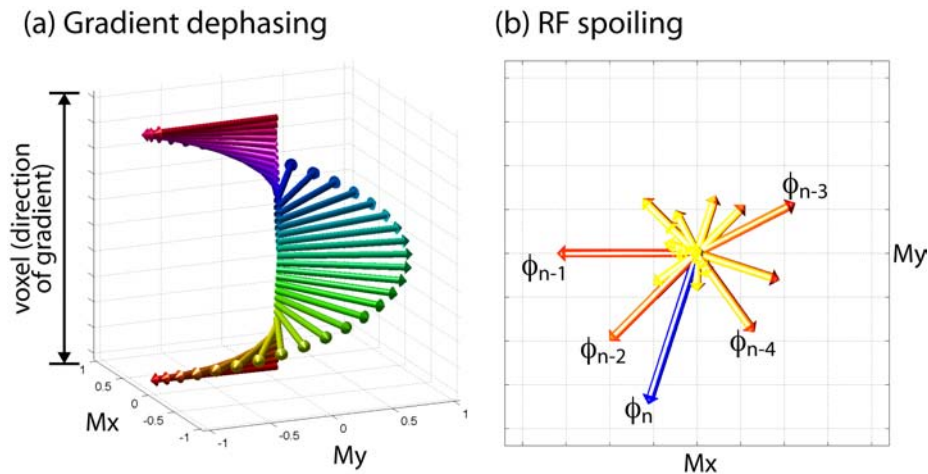


**Figure 2.** Phase manipulation techniques for spoiling residual transverse signal at the end of the TR. (a) Gradient spoiling uses a strong gradient pulse to put a multiple of  $2\pi$  phase across a voxel dimension (here, exactly  $2\pi$ ). Ideally, this will cause the signal across the voxel to cancel; however, this well-organized pattern of phase can easily be reversed by subsequent gradients, causing the magnetization to rephase (align), creating a signal echo. (b) In RF spoiling, magnetization is excited with a varying phase angle ( $\phi_n$  in the  $n$ th TR period). The residual magnetization from previous repetition periods will tend to phase cancel (above, the signals with phase  $\phi_k$ ,  $k < n$ ). While RF spoiling can be thought of as “pseudo-randomizing” the magnetization phase, in practice quadratic schemes are used because they provide a stable signal, unlike purely random phase. Although the gradient scheme in (a) may initially appear to be more robust by exactly canceling transverse signal, in practice RF spoiling (b) is much more powerful.

**RF spoiling.** A more powerful technique for removing the signal contribution from residual transverse magnetization is RF spoiling. The basic idea is to tip the magnetization about a different axis in each TR (i.e., change the RF phase) [3]. The transverse magnetization that is excited in one TR will therefore have a phase angle that is offset relative to the magnetization that persists from prior excitations. If the tip axes are chosen appropriately, fresh signal from the most recent RF pulse will dominate, while residual transverse components will phase cancel (another form of dephasing, see Figure 2b). RF spoiling is often described as “pseudo-randomizing” the phase of the RF pulse, but in fact random phase angles can lead to signal instability [4]. In practice, a quadratic schedule of phase angles has been shown to provide a stable signal. In quadratic phase cycling, the phase for the  $n$ th RF pulse given by  $\phi_n = n(n+1)\Delta\phi$  and constant increment,  $\Delta\phi$ . The effectiveness of RF spoiling in creating pure T1 contrast is critically dependent on the specific phase increment. Suppression of residual transverse magnetization makes the signal approximately independent of T2, resulting in signal that is a relatively pure T1 contrast. A helpful discussion of RF spoiling is given in [5].

### Steady-state free precession (SSFP).

Unlike spoiled sequences, SSFP techniques aim to make use of the residual transverse magnetization at the end of each TR period. These sequences have fixed dephasing gradients and constant (or, in some cases, linearly increasing<sup>1</sup>) RF phase. In order to be in the steady state, the magnetization vector must be identical from one TR to the next. For this constraint to be satisfied, the RF pulse must exactly cancel all sources of motion that the magnetization vector experiences during the TR, thus placing the magnetization vector back where it started [3]. Sources of motion of the magnetization vector include

<sup>1</sup> RF phase often uses a linear schedule (i.e., the phase is  $n\Delta\phi$  in the  $n$ th period, often with  $\Delta\phi = 180^\circ$ ). This can be shown to be equivalent to constant RF phase for magnetization with shifted resonance frequency [6]. This detail is not crucial to a basic understanding of SSFP, and is not discussed further.

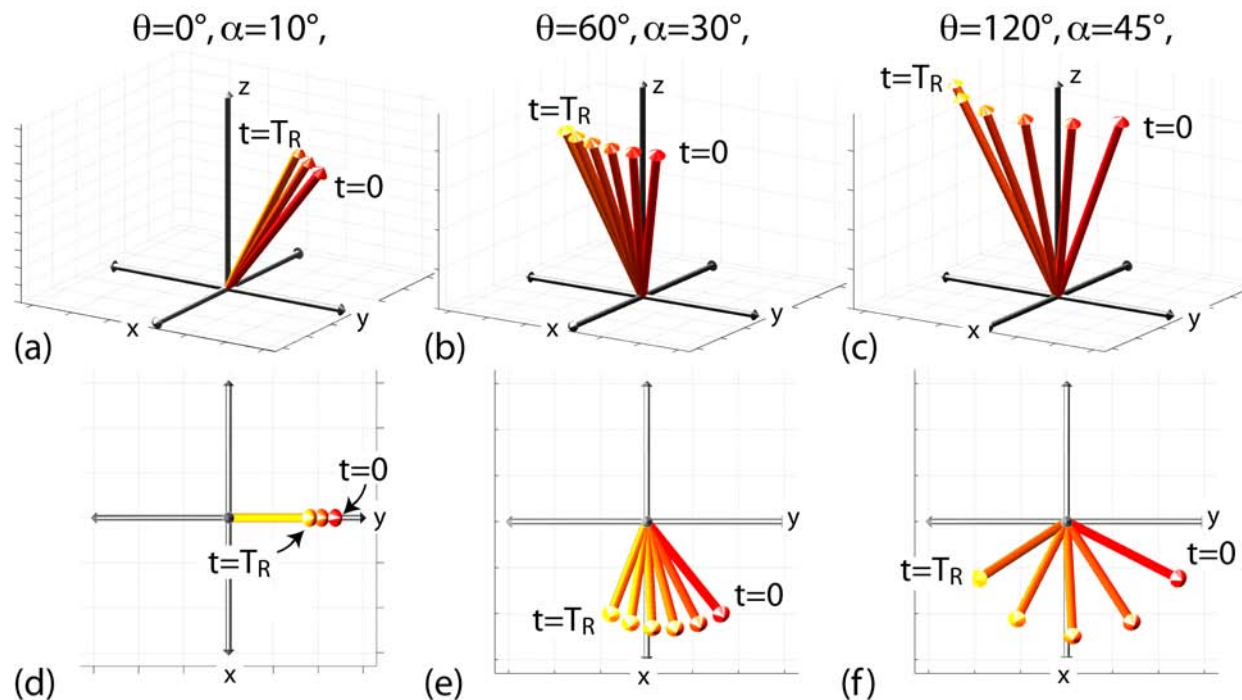


**Figure 3** Steady-state magnetization in an SSFP sequence. Three different conditions are plotted for magnetization vectors that experience different precession angles,  $\theta$  (the same magnetization vectors are plotted in different views in the top and bottom rows). For ease of illustration, each precession angle is shown for the flip angle at which signal is approximately maximized. Each panel shows the progression of the magnetization vector over the course of one TR: it rotates about the z axis due to precession and undergoes relaxation. To be in the steady state, the movement of the magnetization during the TR must be cancelled by the RF pulse (here, about the x axis), which will rotate it back to its starting position. For magnetization that does not precess during the TR (a,d), the RF pulse cancels relaxation only, and the steady state lies in the y-z plane. Magnetization that precesses by a significant amount will have very different behavior (b,c,e,f), with the transverse component sweeping across the x axis during the TR. These simulations used approximate values for brain tissue at 3T ( $T_1/T_2=1300/100$  ms) and a fairly long TR (20 ms) in order to better demonstrate the effects of relaxation. Note that each precession angle is shown here at its optimal flip angle, and all three have very similar signal levels; however, in an image acquired with on particular flip angle, these precession angles will exhibit very different signal levels (see

relaxation (reorienting the vector relative to the transverse plane) and precession (rotating the vector about the longitudinal axis). The  $T_1$ ,  $T_2$ , flip angle and phase angle (due to off-resonance or gradient-induced precession) exactly determine the magnetization vector that satisfies this steady-state condition. Unlike most sequences, in which magnetization dynamics are dominated by relaxation, precession is the dominant effect in SSFP. Balanced and unbalanced SSFP sequences differ in the source of this phase accrual, and in the way signal sums across a voxel.

**Balanced SSFP.** Balanced steady-state free precession (SSFP) has the key characteristic that all gradients are fully refocused (have zero net area) across a repetition period [7]. The only source of phase accrual during the TR is therefore due to off-resonance precession (e.g., precession due to field variations reflecting an imperfect shim). To be in the steady state, rotation due to precession must be cancelled by the RF tip, which causes the steady-state magnetization vectors for different resonance frequencies to differ (see examples in Figure 3). The well-shimmed voxels in typical MRI experiments will be roughly characterized by a single resonance frequency. The intriguing result is that the voxel signal depends on its resonance frequency (see Figure 4), creating image contrast that reflects the local

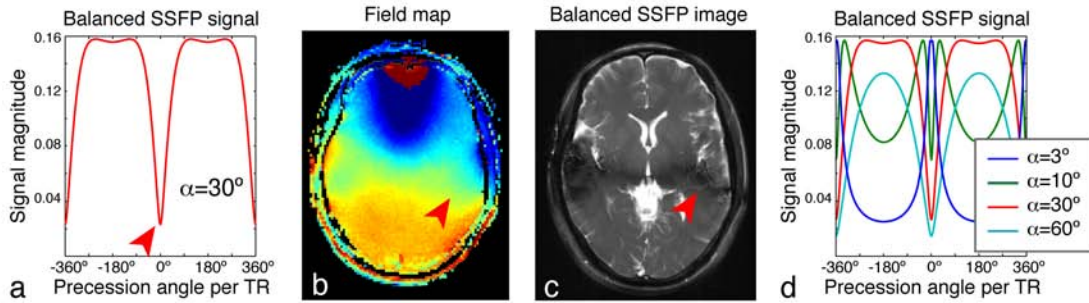


**Figure 4.** (a) The SSFP signal magnitude varies with resonance frequency. Because the magnetic field is never perfectly homogeneous (see fieldmap in b) images exhibit characteristic dark bands (c). Arrows indicate a brain region with resonance frequency corresponding to low signal in the transition band. (d) The dependence of signal magnitude on resonance frequency varies with flip angle. Nevertheless, at all flip angles the signal has its greatest sensitivity at multiples of  $360^\circ$  precession per TR (the “transition band”) and lowest sensitivity at odd multiples of  $180^\circ$  precession (the “pass band”).

magnetic field in addition to T1 and T2 [8]. Although individual voxels are typically well shimmed, the frequency will slowly vary across the brain, creating low-signal regions (“banding artefacts”), as depicted in Figure 4. These bands are often considered artefacts in balanced SSFP imaging, but can also be used as a source of contrast. The SSFP signal profile shown in Figure 4 can be divided into two regions: the transition band, where signal is exquisitely sensitive to small changes in resonance frequency, and the pass band, where it is relatively insensitive to frequency. Since the frequency dependence of the signal is driven by the amount of precession-induced rotation between RF pulses, the distance between transition bands is dependent on the time between pulses, the TR. As the TR changes, the bands remain  $TR^{-1}$  Hz apart. The balanced SSFP signal does nevertheless depend on relaxation, and is often stated to have T2/T1 contrast (provided imaging occurs in the passband with  $TR \ll T2$  and at the optimal flip angle [9]). Finally, there is also a fairly complicated dependence of the signal on flip angle (see Figure 4), a full discussion of which is outside of the scope of this review.

**Unbalanced SSFP.** A second type of SSFP sequence includes an unbalanced gradient pulse [10]. At first glance, the unbalanced sequence in Figure 1c resembles the gradient-spoiled sequence in Figure 1a. The crucial difference is that the gradient “spoiler” in unbalanced SSFP does not vary from one TR to the next. The effects of the gradient pulse during one repetition period can be reversed to re-form signal in subsequent TRs (the details of this signal formation are nicely described in [11]). In terms of signal dynamics, unbalanced SSFP is actually very closely related to balanced SSFP, since the magnetization steady state is determined by net precession during the TR. This phase is constant across a voxel in balanced SSFP, whereas in unbalanced SSFP, this phase angle varies within the voxel. The detected signal in unbalanced SSFP is the summation of the signal across the voxel, i.e., the average of the transverse magnetization shown in Figure 4. The resulting images therefore do not exhibit banding. The final characteristic that affects unbalanced SSFP sequences is whether the gradient occurs before or after the readout. If the gradient occurs after the readout, magnetization that is freshly excited by the RF pulse, the free induction decay (FID), contributes signal, giving rise to one name for this sequence: SSFP-FID. If the gradient occurs before the readout, fresh magnetization is immediately dephased and does not contribute signal, such that all signal comes from “echoes” formed over multiple TRs, and the sequence is an SSFP-Echo.

### Coherence pathways and steady-state imaging.

Retaining the residual transverse magnetization at the end of each TR leads to complicated magnetization behavior. The magnetization can no longer be assumed to lie entirely along the I

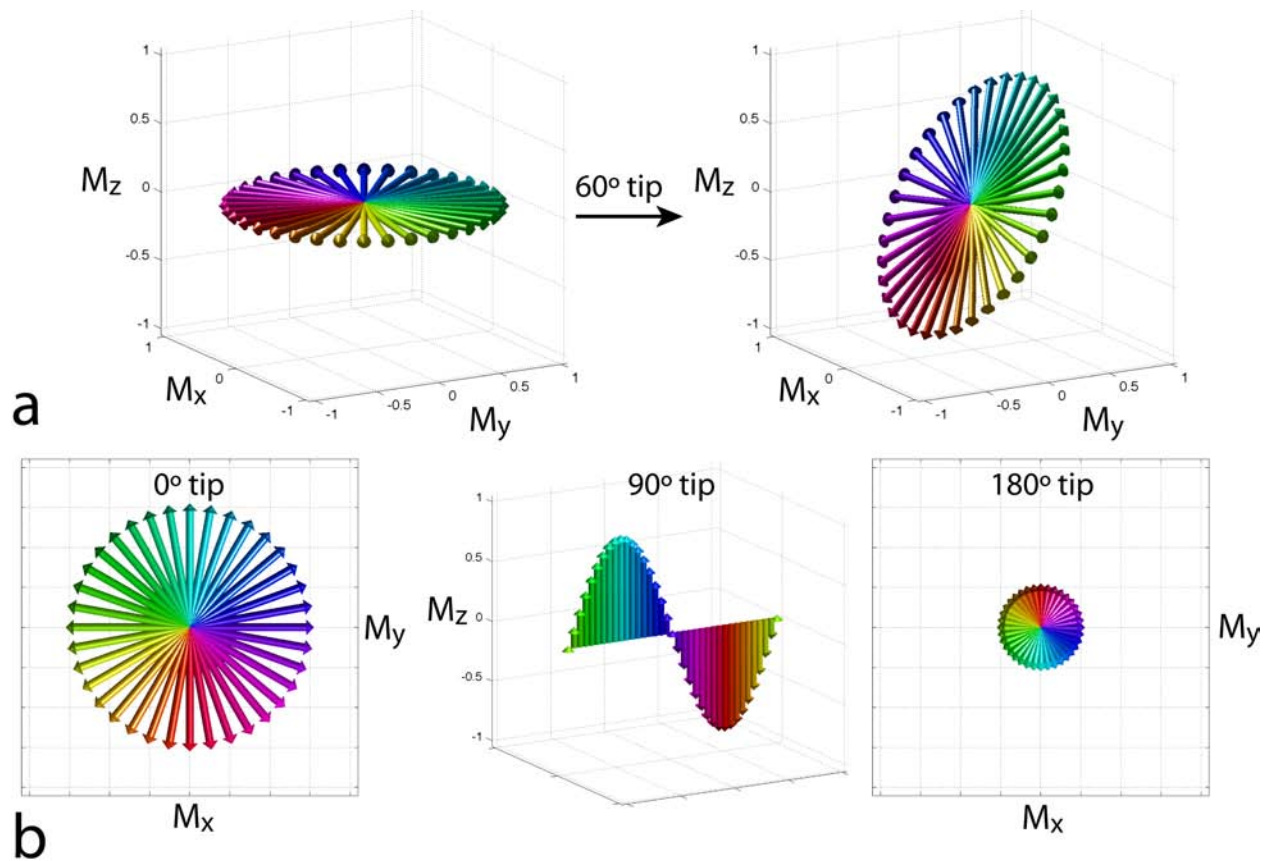


**Figure 5.** The effect of a tip of arbitrary flip angle is equivalent to the combined effect of 0°, 90° and 180° pulses each applied to a subset of the magnetization. For example, a 60° tip about the y axis will tilt any existing transverse magnetization, as shown on the top row. Keeping track of relaxation and precession effects on this distribution becomes extremely complicated after just a few RF pulses. Instead, we break this tilted distribution down into transverse and longitudinal parts. The longitudinal component has effectively seen a 90° pulse, which tipped it from transverse to longitudinal (the magnetization vectors are separated on the middle bottom plot for ease of visualization). The transverse component forms an ellipse (i.e., this is the shape one would see viewing the top right plot from above). While intuitive, this ellipse is a fairly complicated distribution to track. Instead, we will treat the ellipse as the summation of two circles in the transverse plane, one with the same orientation as the original magnetization (0° tip) and one flipped about the y axis (180° tip). Thus, the fairly complicated magnetization distribution can be described by three values: the amount of magnetization that has effectively experienced 0°, 90° and 180° components. These three components then evolve independently according to the Bloch equations.

longitudinal axis at the end of the TR, but rather has some angle to it. In subsequent TRs, the RF pulse will rotate this magnetization, followed relaxation, precession and gradient-induced rotation. Tracking this complicated behavior is a daunting task.

One way to approach these calculations is to use coherence pathways, also known as “phase graphs”. An excellent (and entertaining) discussion of the theory underlying coherence pathways is given by Hennig (2), and further discussion specific to steady-state imaging with short TR is given by Scheffler (3). The basic concept is to consider each RF pulse to act like a composite of 0°, 90° and 180° pulses<sup>2</sup>, as shown in Figure 5. The RF pulse can be considered to “split” the existing magnetization into three

<sup>2</sup> Breaking an  $\alpha < 90^\circ$  pulse into 0° and 90° components may seem intuitive, while a 180° is less intuitive. However, it is simply a mathematical necessity that arises when representing a vector rotating in a 3-dimensional space in terms of a complex transverse component and a scalar longitudinal component.

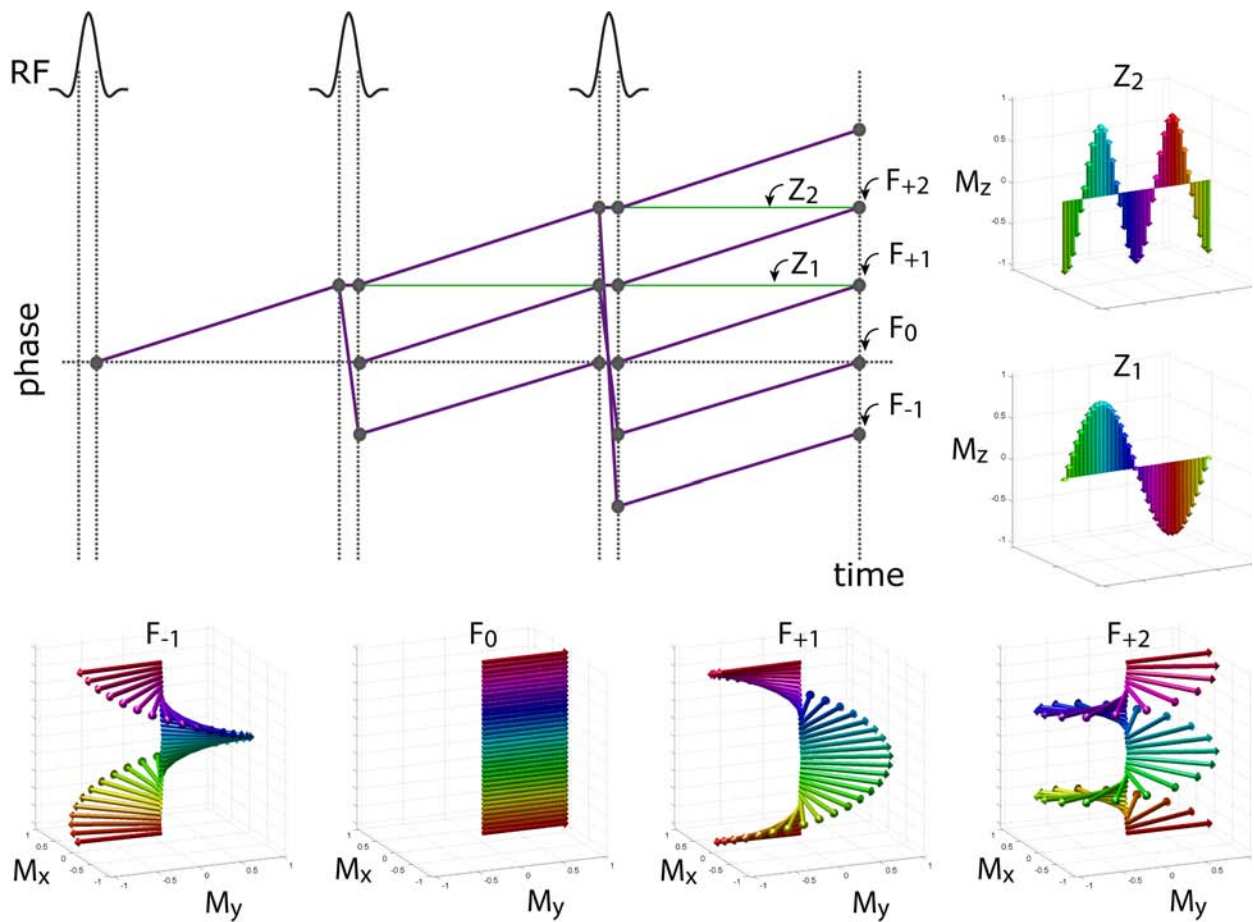


**Figure 6.** Coherence pathway analysis is typically visualized as a plot of magnetization phase vs time. Each RF pulse splits existing magnetization into 3 components, creating a spreading tree of magnetization components. Above, we show the coherence pathway analysis for three RF pulses applied to the equilibrium magnetization,  $M_0$ . The sloped purple lines represent transverse components ( $F_n$ , which accrue phase) and the horizontal green lines represent longitudinal components ( $Z_n$ , which have fixed phase). For simplicity of illustration, we depict phase accruing at a constant rate, although this is often not the case. The distribution of transverse or longitudinal magnetization for several example components is depicted in the 3D vector plots. In SSFP-FID or SSFP-Echo sequences, phase accumulation is driven by the unbalanced gradient, which is chosen to create  $2\pi$  phase across a voxel. In this case, we can think of the depicted states as representing the magnetization across a voxel, and the slope of the lines in the phase plot represent the phase spread across the voxel. All of the high-order transverse ( $F_n$ ) states will self-cancel, and only the  $F_0$  state will contribute signal. For balanced SSFP, the only source of phase accrual is off-resonance precession. In this case, a given voxel would be represented by one of the vectors in the 3D plots, based on the angle of precession-induced phase per TR. In this case, all transverse states contribute signal, and the total signal is the summation across states. It is critical to appreciate that, although our interpretation of the states differ for balanced and unbalanced SSFP, the total magnetization in each state is identical.

components (where the fraction of magnetization that is allocated to each component depends on the flip angle,  $\alpha$ ). A train of pulses splits the magnetization into many coherence pathways, and the total signal is the summation over all coherence pathways.

The appeal of coherence pathways is that, after this splitting, the behavior of each component can then be tracked independently. The magnetization in a given pathway will experience T1 recovery during longitudinal periods and T2 decay during transverse periods. Relaxation dictates that each pathway will

eventually fade away. Most importantly, we have a much simpler way to account for dephasing of the signal during transverse periods.

By tracking dephasing, coherence pathways are able to encapsulate fairly complicated behavior, such as the refocusing of dephased magnetization many TRs after its initial excitation. This kind of refocusing can be considered as a type of spin or stimulated echo. In fact, this represents the general view of steady-state sequences within the coherence pathway framework: the signal we receive is a mixture of free induction decays and (spin and stimulated) echoes, each coming from a single coherence pathway. Because it represents a mixture of signals, this kind of sequence has highly flexible contrast.

While the discussion above considered coherence pathways in the context of short TR imaging, they are also extremely useful to understand experiments with varying TR and flip angles.

### **Properties of steady-state imaging.**

Steady-state sequences span a broad range of imaging strategies and signal mechanisms; however, there are a number of properties of steady-state sequences that differ from more “conventional” sequences. In this section, we describe a few key properties common to steady-state sequences.

**Maintaining the steady state.** One key property of steady-state sequences, which is often invisible to the end user but nevertheless dictates many of the decisions and techniques employed, is the need to achieve and maintain the steady state. The steady state is only established after RF pulses are applied for a duration of about  $3xT_1$ , during which time the signal can be highly unstable. Many techniques that form a part of the conventional MRI sequence toolkit are considerably more difficult to achieve while maintaining the steady state. For example, conventional methods for fat saturation, inversion recovery and flow sensitization would disturb the steady state, necessitating different approaches. One important discovery in steady-state imaging is the ability to “catalyze” the steady state: to apply a series of RF pulses that places the magnetization close to its final steady state [12,13]. Catalyzation reduces transient signal oscillations, thereby enabling acquisition to commence immediately rather than waiting for the steady state to develop [14].

**3D acquisition.** In order to maintain the transverse steady state, we must satisfy the condition that  $TR \leq T_2$ , which in general means  $TR < 50-100$  ms. The use of 2D multi-slice excitations in this range of TR would require us to image slice-by-slice, re-establishing the steady state for each slice in turn, sacrificing the SNR efficiency advantage. Therefore, steady-state sequences almost always utilize 3D, slab-selective k-space acquisitions, acquiring a small subset of 3D k-space each TR. These acquisitions are highly SNR efficient and tend to have low image distortion. However, they also are sensitive to certain sources of artefact, such as motion and flow, and preclude some options such as inter-slice gaps. Several groups have proposed flow- and motion-compensation schemes for cardiac imaging (for example, [15,16]), but these methods remain largely unexplored in the brain.

**Low flip angle.** Conventional sequences with long TR often use  $90^\circ$  excitation pulses to maximize signal. However, for short TR, signal can actually increase at lower flip angle (with the optimum often referred to as the “Ernst angle”). This is particularly true for the range of TR used in steady-state sequences, where the maximum signal is often achieved with flip angles of  $30-40^\circ$ . In addition, many of the steady-state techniques described below (e.g., fMRI and diffusion imaging) achieve optimal contrast (as distinct from optimal signal) at much lower flip angles of  $5-30^\circ$ . One consequence of this is that steady-state methods often have low RF energy deposition, even though RF pulses may be applied rapidly. However, the use of TR on the order of  $2-5$  ms does mean that flip angles as low as  $60^\circ$  can be constrained by energy deposition, even at  $3T$ .

**High SNR efficiency.** The key property defining steady-state sequences is the use of very short TR, and these sequences are often described as “rapid imaging”. In practice, steady-state sequences do not necessarily have short acquisition times (i.e., 3D image formation can take minutes), but they are characterized by very efficient acquisitions [17]. This property arises due to the similar timescale of the TR and typical k-space readouts: milliseconds to tens of milliseconds. Most steady-state sequences therefore allow the majority of the TR to be dedicated to acquiring data. This allows steady-state sequences to overcome the very low intrinsic signal levels caused by short TR. Although the baseline signal that is acquired can be as low as  $5-15\%$  of  $M_0$ , the efficiency of the readout (occupying  $60-90\%$  of the TR) will often more than make up for this in the final SNR of the image. The SNR efficiency of spoiled steady-state sequences is considerably lower, despite similar TRs. These sequences do not re-

use the transverse magnetization over multiple TR periods and therefore have drastically reduced baseline signal (up to 5 times less signal than SSFP sequences).

**Complicated signal dependence.** One of the biggest challenges with steady-state sequences is that increased efficiency comes at the cost of a more complicated signal. As mentioned above, the signal in steady-state sequences is in general sensitive to T1, T2 and phase accrual. With the proper tools for understanding this behavior, this complexity can lead to a fascinating degree of flexibility and interesting signal behavior. However, this complicated dependence is also a critical confound to unambiguously interpreting the signal in steady-state images.

1. Haase A, Frahm J, Matthaei D, Hanicke W, Merboldt KD. FLASH imaging. Rapid NMR imaging using low flip-angle pulses. *J Magn Reson*, 67, 258-266 (1986).
2. Crawley AP, Wood ML, Henkelman RM. Elimination of transverse coherences in FLASH MRI. *Magn Reson Med*, 8, 248-260 (1988).
3. Freeman R, Hill HDW. Phase and Intensity Anomalies in Fourier Transform NMR. *J Magn Reson* 4, 366-383 (1971).
4. Zur Y, Wood ML, Neuringer LJ. Spoiling of transverse magnetization in steady-state sequences. *Magn Reson Med*, 21, 251-263 (1991).
5. Bernstein MA, King KF, Zhou XJ. *Handbook of MRI pulse sequences* (Elsevier, 2004).
6. Zur Y, Stokar S, Bendel P. An Analysis of Fast Imaging Sequences with Steady-State Transverse Magnetization Refocusing. *Magn Reson Med* 6(2), 175-193 (1988).
7. Carr HY. Steady-State Free Precession in Nuclear Magnetic Resonance. *Phys Rev Lett*, 112, 1693-1701 (1958).
8. Oppelt A, Graumann R, Barfuss H, Fischer H, Hartl W, Shajor W. FISP- A new Fast MRI Sequence. *Electromedica*, 54, 15-18 (1986).
9. Scheffler K, Lehnhardt S. Principles and applications of balanced SSFP techniques. *European radiology*, 13(11), 2409-2418 (2003).
10. Gyngell M. The application of steady-state free precession in rapid 2DFT NMR imaging: FAST and CE-FAST sequences. *Magn Reson Imaging*, 6, 415-419 (1988).
11. Hennig J. Echoes: How to generate, recognize, use or avoid them in MR-imaging sequences. *Concepts Magn Reson* 3, 125-143 (1991).
12. Deimling M, Heid O. Magnetization prepared true FISP imaging. In: *Proc 2nd ISMRM*. (Ed.^(Eds) (San Francisco, 1994) 495.
13. Nishimura DG, Vasanawala S. Analysis and reduction of the transient response in SSFP imaging. In: *Proc 8th ISMRM*. (Ed.^(Eds) (Denver, 2000) 301.
14. Hargreaves BA, Vasanawala SS, Pauly JM, Nishimura DG. Characterization and Reduction of the Transient Response in Steady-State MR Imaging. *Magn Reson Med* 46(1), 149-158 (2001).
15. Bieri O, Scheffler K. Flow compensation in balanced SSFP sequences. *Magn Reson Med*, 54(4), 901-907 (2005).
16. Storey P, Li W, Chen Q, Edelman RR. Flow artifacts in steady-state free precession cine imaging. *Magn Reson Med* 51, 115-122 (2004).
17. Ernst R, Anderson W. Application of Fourier transform spectroscopy to magnetic resonance. *Review of Scientific Instruments*, 37, 93-102 (1966).